

Analysis of Radiation-Induced Cell Death in HNSCC and Rat Liver Maintained in Microfluidic Devices.

Carr S¹ BSc(Hons) MRCS DOHNS, Green VL² BSc(Hons) PhD,
Stafford ND¹ FRCS (ORL-HNS), Greenman J² BSc(Hons) PhD

¹Hull York Medical School

²School of Biological, Biomedical & Environmental Sciences, Daisy Research
Laboratories,
University of Hull, HU6 7RX

Oral Presentation:

American Academy of Otolaryngology – Head and Neck Surgery Foundation
Conference, Washington DC, September 2012

Corresponding Author:

Mr. Simon Carr

Daisy Research Laboratories, University of Hull, Hull, UK, HU6 7RX

E-mail: simoncarr15@gmail.com

Keywords:

Microfluidic techniques; Radiotherapy; Head and neck squamous cell carcinoma; Rat liver

Abstract

Objective

The aim of this study was to investigate how HNSCC tissue biopsies maintained in a pseudo *in vivo* environment within a bespoke microfluidic device, respond to radiation treatment.

Study Design

Feasibility study.

Setting

Tertiary referral centre.

Subjects and Methods

35 patients with HNSCC were recruited, in addition liver tissue from 5 Wistar rats. A microfluidic device was used to maintain the tissue biopsy samples in a viable state. Rat liver was used to optimise the methodology. HNSCC was obtained from patients with T1-T3 laryngeal or oropharyngeal SCC; N1-N2 metastatic cervical lymph nodes were also obtained. Irradiation consisted of single doses of between 2Gy and 40Gy and a fractionated course of 5x2Gy. Cell death was assessed in the tissue effluent using the soluble markers LDH and cytochrome c, and in the tissue by immunohistochemical detection of cleaved cytokeratin18 (M30 antibody).

Results

A significant surge in LDH release was demonstrated in the rat liver after a single dose of 20Gy; in HNSCC it was seen after 40Gy compared to the control. There was no significant difference in cytochrome c release after 5Gy or 10Gy. M30 demonstrated a dose-dependent increase in apoptotic index for a given increase in single dose radiotherapy. There was a significant increase in apoptotic index between 1x2Gy and 5x2Gy.

Conclusion

M30 is a superior method compared to soluble markers in detecting low-dose radiation-induced cell death.

This microfluidic technique can be used to assess radiation-induced cell death in HNSCC and therefore has the potential to be used to predict radiation response.

Introduction

Head and neck squamous cell carcinoma (HNSCC) accounted for 2.8/100,000 of all cancers in the UK in 2011 and represents the seventh most common cancer in Europe ¹. Globally, it is the sixth commonest form of cancer with an incidence of 700,000 cases per year ².

Radiotherapy is used as a single modality treatment for early stage laryngeal cancer (T1 and T2) and in conjunction with chemotherapy in T3 laryngeal and oropharyngeal SCC. However, up to 25% of early stage laryngeal SCC are radioresistant ³. The ability to predict radioresistance would prevent patients undergoing a potentially unnecessary treatment with its significant associated morbidity. The only curative option after radiotherapy failure is salvage surgery, which is associated with a poorer functional outcome and a prolonged hospital stay ⁴ adding to the significant time and cost implications to the health service.

There are three modes of radiation-induced cell death, all of which are secondary to DNA damage: apoptosis, mitotic catastrophe, which leads to caspase-dependent (apoptotic) or caspase-independent (necrotic) cell death ⁵, and senescence, a form of proliferative stasis ⁶. In HNSCC, it has been shown that radiotherapy induces all three modes of cell death, with the majority of cells undergoing mitotic catastrophe and senescence, although apoptosis plays a major role ⁷. Apoptosis can be measured using a range of *in vitro* techniques, including soluble and tissue markers. The soluble markers used in this study to determine the effects of radiation treatment on HNSCC tissue maintained in a microfluidic device were lactate dehydrogenase (LDH), an intracellular enzyme, and cytochrome c, which is stored in the mitochondria and is responsible for the stimulation of caspases as part of the apoptotic cascade; both of these factors are released from membrane compromised cells. Immunohistochemistry

was used to detect caspase-3 cleaved cytokeratin 18 using the M30 antibody, which is a tissue marker of apoptosis.

Microfluidic devices provide a simple, reproducible and highly versatile system for maintaining tissue biopsies, allowing the tissue to remain viable and functional by preserving the three-dimensional architecture and its *in vivo* microenvironment^{8,9,10}.

This microenvironment enables cell-cell and cell-matrix interactions to be maintained¹¹, which govern the behaviour of tumour cells. These interactions include subcellular signalling, chemotaxis, proliferation, differentiation and death¹², essential processes in determining the cellular response to radiotherapy.

The aim was to use a simple microfluidic device to detect the radiation-induced cell death of HNSCC biopsy samples, with the ultimate goal being the development of a tool capable of predicting the response of a patient's HNSCC to radiotherapy on an individual basis prior to the commencement of treatment.

Methods

The microfluidic device

The microfluidic device used in this feasibility study was fabricated from two layers of glass, thermally bonded together. The upper layer had one inflow and two outflow holes, which corresponded to channels etched into the lower layer. The tissue was accommodated in a central well over which a microport (Anachem, UK) was bonded. An English-threaded adaptor (Anachem, UK), filled with poly-dimethylsiloxane (PDMS; Dow Corning, UK) was screwed into the microport to seal the chamber and to allow gaseous exchange¹³.

The microfluidic system

A 20ml syringe filled with Dulbecco's Modified Eagles Medium (DMEM; 10% (w/v) FBS, 3% (w/v) HEPES (PAA, UK), 1% penicillin/streptomycin (Sigma, UK), 1% (w/v) NEAA (PAA, UK) and 1% (w/v) glutamine) was placed into a Harvard PhD 2000 syringe pump (Harvard, UK) and connected to the microfluidic device using a three-part adaptor (Upchurch Scientific, WA, USA) and TFE Teflon® tubing (Anachem, UK). A 0.22µm filter (Millipore, UK) was fitted in-line to prevent bacterial contamination and minimise bubble formation. Trimmed 200µl pipette tips (Sarstedt, UK) connected the tubing to the device. The device and tubing were maintained at 37°C inside an incubator. Medium was flowed over the tissue at a rate of 2µl min⁻¹ and the effluent was collected at 2-hourly intervals and stored at 4°C for use in subsequent assays.

Tissue preparation

Rat liver was used to optimise the methodology, as it was homogeneous, highly metabolically active and moderately radiosensitive, similar to HNSCC^[1]. The liver was harvested from 5 Wistar rats that were fed and watered *ad libitum* until anaesthetized (10ml kg⁻¹ of 10mM sodium thiopentone, intraperitoneal) and killed under a Schedule 1 procedure by a trained animal technician.

Samples of HNSCC were provided in accordance with Local Research Ethics Committee (LREC-10/H1304/6;AM01) and NHS Trust R&D approval (R0987) from a cohort of 35 patients undergoing surgery at Castle Hill Hospital, Hull with no history of previous treatment, with either laryngeal or oropharyngeal SCC tumours staged at T1-T3; metastatic lymph nodes staged at N1-N2 were also collected. It took approximately 30-40 min to place the tissue in the device after resection.

Tissues were transported to the laboratory in DMEM at 4°C and were either immediately divided into approximately 3mm³ sections, each weighing 5-10mg and placed into the device or snap frozen in liquid nitrogen and stored at -80°C for future use.

During each experiment two controls were used consisting of HNSCC or rat liver tissue from the same sample: tissue not incubated in the device and tissue that was not irradiated, but was incubated in the device for the same duration as the irradiated sample. Both fresh and frozen tissue samples were used, as a previous study had demonstrated no significant difference in the tissue response between the two groups following interrogation in the microfluidic device¹³.

Radiotherapy treatment

Irradiation was performed using a 6 MV photon beam from a Varian Linear Accelerator. To ensure delivery of an accurate and uniform dose, the microfluidic device was housed inside a perspex phantom (**Figure 1**). CT planning calculated that at gantry angles of 90° and 270° with a 5cm x 5cm field, each beam delivered 114 MU, which produced a dose of 2Gy to the centre of the tissue, increased as necessary to achieve the required dose.

Radiotherapy was administered to the tissue after at least 24 h incubation in the microfluidic device. A single dose of 20Gy was administered to the rat liver. Single doses of between 2Gy and 40Gy, and a fractioned course of 5x2Gy over a 5-day period, which reflected a clinical weeklong radiotherapy course, were administered to the HNSCC tissue.

Lactate dehydrogenase and cytochrome c assays

LDH and cytochrome c were measured in the effluent collected from the microfluidic device using the LDH cytotoxicity kit plus (Roche Diagnostics, UK) and the Quantikine® human cytochrome c immunoassay kit (R&D Systems, UK) respectively; both used according to the manufacturer's protocol. A lysis agent (10% v/v Triton-X (Cytotoxicity Detection Kit (LDH), Roche, UK) was added in certain experiments prior to the end of the experiment to indicate if live tissue still remained.

Immunohistochemistry

The tissue was removed from the device 72 h after irradiation for the single dose regimens and 4 h after the final dose in the fractionated course. Once the tissue was removed, it was fixed with Tissue-Tek (Sakura, UK), and snap frozen in liquid nitrogen-cooled 2-methyl-butane (Sigma, UK) and stored at -20°C. The tissue was subsequently cut into 8-10µM sections using a cryostat and mounted onto poly-L-lysine coated slides (SLS, UK).

M30 CytoDEATH™ (Peviva, UK) is a monoclonal antibody, which detects caspase-3 cleaved cytokeratin-18 as a specific marker of apoptosis. Tissue sections were fixed in methanol before washing in Tris-buffered saline. Endogenous peroxidase activity was blocked with 3% H₂O₂ in methanol for 15 minutes. The Vectastain Elite Universal horseradish peroxidase Kit (Vector, UK) was used as directed. Non-specific avidin-biotin binding was blocked by incubating with Avidin D followed by Biotin (Vector Laboratories, UK) for 15 minutes each. The M30 CytoDEATH™ (Peviva, UK) antibody was used at a dilution of 1:100 for 1 hour at room temperature. The location of antibody was detected using diaminobenzidine (Sigma, UK), before the sections were counterstained with hematoxylin, dehydrated through graded alcohols (70%, 90%, 100%) and histoclear and mounted in Histomount (National Diagnostics, UK).

Calculation of the Apoptotic Index

The apoptotic index (AI) was calculated by counting the number of cells that stained positive for M30 in ten randomly chosen high-power fields; only fields that contained positive cells were selected. The number of M30-positive cells was expressed as a percentage of the total number of cells in that field. A total of approximately 3000 cells were counted in ten fields ¹⁴.

Statistical Analysis

Statistical analysis was performed using SPSS (IBM, USA). The unpaired t-test was used to determine the statistical significance between treatments. *P*-values <0.05 were considered significant.

Results

LDH and Cytochrome c release

LDH was measurable in the effluent from the microfluidic device as a result of cell death. **Figure 2** shows the levels of LDH released from rat liver (n=3), maintained in the microfluidic device without radiation treatment over a period of 341 hours (15 days); the same trend was observed in the HNSCC tissue (n=3, data not shown). The initial elevated LDH levels decreased to minimally detectable levels 24-28 hours after placement of the tissue into the microfluidic device. LDH levels remained low until lysis agent was added to the culture medium at 333 hours, which induced a subsequent rise in LDH release 2-8 h after its addition.

Administration of a single dose of 20Gy to the rat liver (n=3), 24 h after the tissue was placed in the device caused a significant increase in LDH release during the 2 h post-irradiation period compared to the non-irradiated control (**Figure 3**). The LDH levels subsequently dropped until the lysis agent was added at 70 h to the irradiated and control tissue, after which a significant ($p=0.02$) rise in LDH was demonstrated; the LDH levels being lower in the irradiated group compared to the control.

Following on from the rat liver experiments, single doses of radiation were administered to the HNSCC tissue (n=3 for each dose). A significant increase in LDH ($p=0.01$) release 2 h after irradiation was detected after the tissue (T1N2b tonsil, T3N2b larynx and T2N2b tonsil metastases) was treated with a single dose of 40Gy at 52 h, whereas treatment with 10Gy at 52 h (T1N2b tonsil, T0N2a metastases and T3 larynx primary) or 5Gy (same HNSCC tissue as 10Gy) and 20Gy at 28 h (same HNSCC tissue as 40Gy) produced no significant increase (**Figure 4a & 4b**).

In order to determine whether apoptosis could be detected in the effluent following the administration of a lower, more clinically relevant dose of radiotherapy (5 and

10 Gy), the apoptotic-specific marker cytochrome c was measured. The pattern of release was similar to that of LDH with initial high levels decreasing after 22 h (data not shown). No statistically significant increase in cytochrome c was observed in the group treated with 5Gy (n=2; T2N2; oropharyngeal metastases) or 10Gy (n=2; T2N2 oropharyngeal metastases) compared with the control measured for at least 72 h following irradiation ($p=0.971$; data not shown).

Detection of cleaved cytokeratin 18

The AI was calculated using M30, an apoptotic-specific antibody, which detects caspase-3-cleaved cytokeratin 18, for the HNSCC tissue following the administration of single doses of 5Gy, 10Gy, 20Gy and 40Gy (n=3 for each dose) and the fractionated radiotherapy course (single dose of 2Gy cf 5x2Gy).

The AI of the HNSCC tissue which had not been maintained in the device and that of the incubated, untreated tissue was below 2% with no significant difference between them (**Figure 5a & 5b**; $p=0.29$). The AI of the irradiated group was significantly higher compared to the non-irradiated tissue incubated in the microfluidic device at all doses ($p=0.006$) and a dose-dependent relationship was observed between the dose of radiotherapy administered and the AI with an increase in radiotherapy dose resulting in an increase in apoptosis.

A significant increase in the AI was observed between the non-irradiated and the irradiated tissue following both the single 2Gy dose (n=3; T1N2c tonsil, T0N2b and T2N2b tonsil metastases) and the fractionated radiotherapy course (5x2Gy; n=3; same HNSCC tissue as single dose of 2Gy; $p=0.002$) and also between the single 2Gy dose and the fractionated (5x2Gy) dose (**Figure 6a & 6b**; $p=0.01$).

Discussion

This proof of concept study used rat liver to optimise the technique and then analysed a series of 35 HNSCC samples to generate data on patient tissue from which appropriately-powered studies can subsequently be devised. The microfluidic device used in this study proved to be an excellent platform for maintaining both rat liver and HNSCC tissue in a pseudo *in vivo* environment over a number of days to allow the effects of radiotherapy to be investigated. Microfluidic techniques have been used previously to maintain HNSCC cells and tissue^{13,15,16,17,18,19,20,21} as well as other tumour types. However, this is the first time that it has been used to study the effects of radiotherapy.

The tissue used in these experiments all proved to be sensitive to radiation. Both rat liver and HNSCC tissue released increased levels of LDH over the first 24 h of incubation caused by tissue handling and dissection during the preparation stage, which has been demonstrated previously^{10,13}. LDH levels in the effluent subsequently decreased to minimally detectable levels at 24-28 h, until the lysis agent was added to the medium, which caused a subsequent LDH increase. The lysis agent caused maximal cell membrane rupture, releasing LDH from any remaining live cells, indicating intact, viable cells within the tissue following maintenance in the microfluidic device for up to 15 days. This is almost double the length of time that tissue has previously been maintained in this device^{10,13}, demonstrating its potential for assessing tissue response to radiation and other tissue interrogation methods over a prolonged time period.

LDH is a marker of both apoptotic and necrotic cell death²² and is an established marker of radiation-induced cytotoxicity^{23,24,25}. Hattersley et al¹³ demonstrated the detection of chemotherapy-induced cytotoxicity using both LDH and cytochrome c

release from HNSCC tissue, which was cultured in an identical microfluidic device to that used in this study. However, this is the first study to demonstrate that LDH measured in the effluent could be used as a marker of radiation-induced cytotoxicity. The administration of a single dose of 20Gy to the rat liver induced a significant level of cell death. The increase in LDH release observed after the addition of the lysis agent indicated the presence of viable cells within the irradiated tissue. The reduced LDH levels in the irradiated tissue compared to the non-irradiated confirmed that a proportion of the cells had perished following irradiation. Although not significant, the reduced LDH levels in the irradiated tissue would indicate that there were fewer remaining viable cells compared to the control.

Several devices were used to assess the effects of different doses of radiation in the HNSCC tissue. The devices were essentially identical up to 28 h; any differences in LDH release represented inter-sample variation. After 52h, a second set of previously untreated devices were irradiated with either 10Gy or 40Gy. Unfortunately, some of the devices following irradiation (20Gy in **Figure 4**) did not maintain tissue throughout the full incubation period, as demonstrated by the decrease in LDH levels. In contrast, HNSCC tissue treated with 5Gy at 28 h continued to produce minimally detectable levels of LDH throughout the experiment.

Over the timescales of the experiments in which the HNSCC tissue was irradiated with single doses of radiation (10Gy or 40Gy), no change in the viability of the HNSCC tissue at later time-points was observed. A total of forty experiments were performed on rat liver and HNSCC tissue (data not shown), which demonstrated the maintenance of tissue viability. The higher radiation doses were administered at later time-points simply due to the logistics of obtaining access to the irradiation source

when fresh HNSCC tissue was available and to provide some degree of standardisation.

Although LDH release could be detected following irradiation of HNSCC tissue, a dose of 40Gy was required to achieve a significant release. The increased dose required in the HNSCC tissue to achieve a significant level of cell death could have been due to a difference in the innate radiosensitivity of these two tissues. After 40Gy, the LDH release could have been detecting a high level of apoptosis or, alternatively, necrosis. Cai et al ²⁵ concluded similarly in their study of the effects of radiotherapy on central nervous system cells after they demonstrated a significant increase in LDH release only after 60Gy.

In this study, both tissues consistently demonstrated a significant surge in LDH release in the 2 h post-irradiation period followed by a sharp decrease. Rao et al ²⁶ demonstrated the same trend after treating HeLa cells with doses of between 1Gy and 4Gy.

Although apoptosis has been identified in microfluidic tissue effluents following the administration of chemotherapeutic agents using cytochrome c ¹³, it has not been used to detect radiation-induced cell death *in vitro*. Cytochrome c could not be detected following the administration of clinically relevant doses of radiation (5Gy and 10Gy). These results, together with the LDH results, indicated that soluble markers were not the best method of detecting radiation-induced cytotoxicity in HNSCC at clinically relevant radiotherapy doses.

The M30 antibody detects an early apoptotic marker and was able to detect radiation-induced cell death after the administration of only 2Gy, the dose of a single fraction used in HNSCC treatment. It could be proposed that M30 also detected those cells undergoing caspase-dependent death as a consequence of mitotic catastrophe. The AI

increased with increasing single doses of radiotherapy and also with an increase in the number of fractions of radiotherapy, providing evidence that this microfluidic technique can be used to investigate the radiosensitivity of HNSCC.

Previous studies using HeLa-Hep2 adenocarcinoma cells have demonstrated the use of M30 as a marker of radiation-induced apoptosis after low-dose radiotherapy.

Mirzaie-Joniani et al ²⁷ used it in their study which showed a significant increase in apoptosis after 2Gy with approximately 20% of the remaining population displaying apoptotic staining at 24 h, whilst Eriksson et al ²⁸ used it to demonstrate increased apoptotic cell death after the combination of low-dose radiation and

radioimmunotherapy. Only Skoda et al ²⁹ have used it in HNSCC, using it with the cell line SCC9 to demonstrate an increased cytotoxicity when Mcl-1 antisense oligonucleotide was used in conjunction with paclitaxel, cetuximab and gemcitabine.

This study has successfully demonstrated that this microfluidic technique can be used to study the effect of radiation on HNSCC tissue. The device was capable of maintaining the HNSCC tissue in a viable state, without it undergoing significant apoptosis and can be used to demonstrate the relationship between radiotherapy dose and radiation-induced cell death using tissue-based markers of apoptosis. The next stage will be to correlate the *in vitro* results with the clinical response of patients to radiotherapy; the ultimate aim being to produce a device that can predict a patient's response to radiotherapy prior to commencement of treatment.

Acknowledgements

We would like to thank Mr. J. Jose, Consultant Head and Neck Surgeon and the rest of the surgical team at Castle Hill Hospital, Hull for providing us with the tissue samples, Dr. L. Karsai, Consultant Histopathologist, Castle Hill Hospital, Hull for his assistance in assessing the sectioned tissue specimens and Dr. G. Liney, Senior Radiotherapy Physicist for his assistance with the radiation treatments.

References

1. Jemal A et al. Global cancer statistics. *CA Cancer J Clin* 2011; 61: 69-90
2. Parkin DM et al Estimating the world cancer burden: Globocan 2000. *Int J Cancer* 2001; 94: 153-6
3. Fernberg JO et al. Radiation therapy in early glottis cancer. Analysis of 177 consecutive cases. *Acta Otolaryngol* 1989; 108: 478-81
4. Withrow KP et al. Free tissue transfer to manage salvage laryngectomy defects after organ preservation failure. *Laryngoscope* 2007; 117: 781-4
5. Mansilla S, Priebe W, Portugal J. Mitotic catastrophe results in cell death by caspase-dependent and caspase-independent mechanisms. *Cell Cycle* 2006; 5: 53-60
6. Eriksson D, Stigbrand T. Radiation-induced cell death mechanisms. *Tumour Biol* 2010; 31: 363-72
7. Ianzini F et al. Lack of p53 function promotes radiation-induced mitotic catastrophe in mouse embryonic fibroblast cells. *Cancer Cell Int* 2006; 6: 11
8. Lee P et al. Microfluidic alignment of collagen fibers for in vitro cell culture. *Biomed Microdevices* 2006; 8: 35-41
9. Nevill JT et al. Integrated microfluidic cell culture and lysis on a chip. *Lab Chip* 2007; 7: 1689-95
10. Hattersley SM, Greenman J, Haswell SJ. Study of ethanol induced toxicity in liver explants using microfluidic devices. *Biomed Microdevices* 2011; 13: 1005-14
11. Young EW, Beebe DJ. Fundamentals of microfluidic cell culture in controlled microenvironments. *Chem Soc Rev* 2010; 39: 1036-48

12. Kamotani Y et al. At the interface: advanced microfluidic assays for study of cell function. *BioMEMS and Biomedical Nanotechnology*. Eds. Ferrari M, Desai T, Bhatia S 2007 Springer US p.55-78
13. Hattersley SM et al. A microfluidic system for testing the responses of head and neck squamous cell carcinoma tissue biopsies to treatment with chemotherapy drugs. *Ann Biomed Eng* 2012; 40: 1277-88
14. Burcombe R et al. Evaluation of Ki-67 proliferation and apoptotic index before, during and after neoadjuvant chemotherapy for primary breast cancer. *Breast Cancer Res* 2006; 8: R31
15. Mauk MG et al. Lab-on-a-chip technologies for oral-based cancer screening and diagnostics: capabilities, issues and prospects. *Ann N Y Acad Sci* 2007; 1098: 467-75
16. Weigum SE et al. Cell-based sensor for analysis of EGFR biomarker expression in oral cancer. *Lab Chip* 2007; 7: 995-1003
17. Ziober BL et al. Lab-on-a-chip for oral cancer screening and diagnosis. *Head Neck* 2008; 30: 111-21
18. Remmerbach TW et al. Oral cancer diagnosis by mechanical phenotyping. *Cancer Res* 2009; 69: 1728-32
19. Mamouni J, Yang L. Interdigitated microelectrode-based microchip for electrical impedance spectroscopic study of oral cancer cells. *Biomed Microdevices* 2011; 13: 1075-88
20. Mulhall HJ et al. Cancer, pre-cancer and normal oral cells distinguished by dielectrophoresis. *Anal Bioanal Chem* 2011; 401: 2455-63
21. Ma H, Zhang M, Qin J. Probing the role of mesenchymal stem cells in salivary gland cancer on biomimetic microdevices. *Inegr Biol (Camb)* 2012; 4: 522-30
22. Kroemer G et al. Classification of cell death: recommendations of the nomenclature committee on cell death 2009. *Cell Death Differ* 2009; 16: 3-11
23. Ts'ao C, Molteni A, Taylor JM. Injury-specific cytotoxic response of tumour cells and endothelial cells. *Pathol Res Pract* 1996; 192: 1-9
24. Reddy AC, Lokesh BR. Effect of curcumin and eugenol on iron-induced hepatic toxicity in rats. *Toxicology* 1996; 107: 39-45
25. Cai L et al. Metallothionein induction in human CNS in vitro: neuroprotection from ionising radiation. *Int J Radiat Biol* 2000; 76: 1009-17

26. Rao SK, Rao PS. Alteration in the radiosensitivity of HeLa cells by dichloromethane extract of guduchi (*Tinospora cordifolia*). *Integr Cancer Ther* 2010; 9: 378-84
27. Mirzaie-Joniani H et al. Apoptosis induced by low-dose and low-dose-rate radiation. *Cancer* 2002; 94: 1210-4
28. Eriksson D et al. Combined low dose radio- and radioimmunotherapy of experimental HeLa Hep 2 tumours. *Eur J Nucl Med Mol Imaging* 2003; 30: 895-906
29. Skoda et al. Down-regulation of Mcl-1 with antisense technology alters the effect of various cytotoxic agents used in treatment of squamous cell carcinoma of the head and neck. *Oncol Rep* 2008; 19: 1499-503

Figures

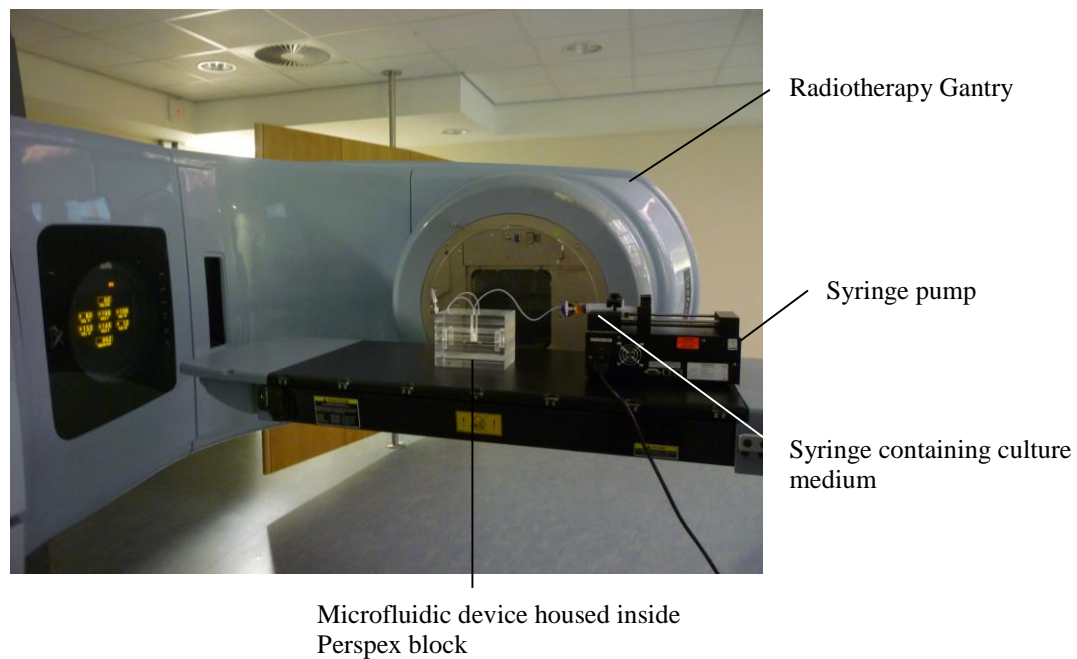
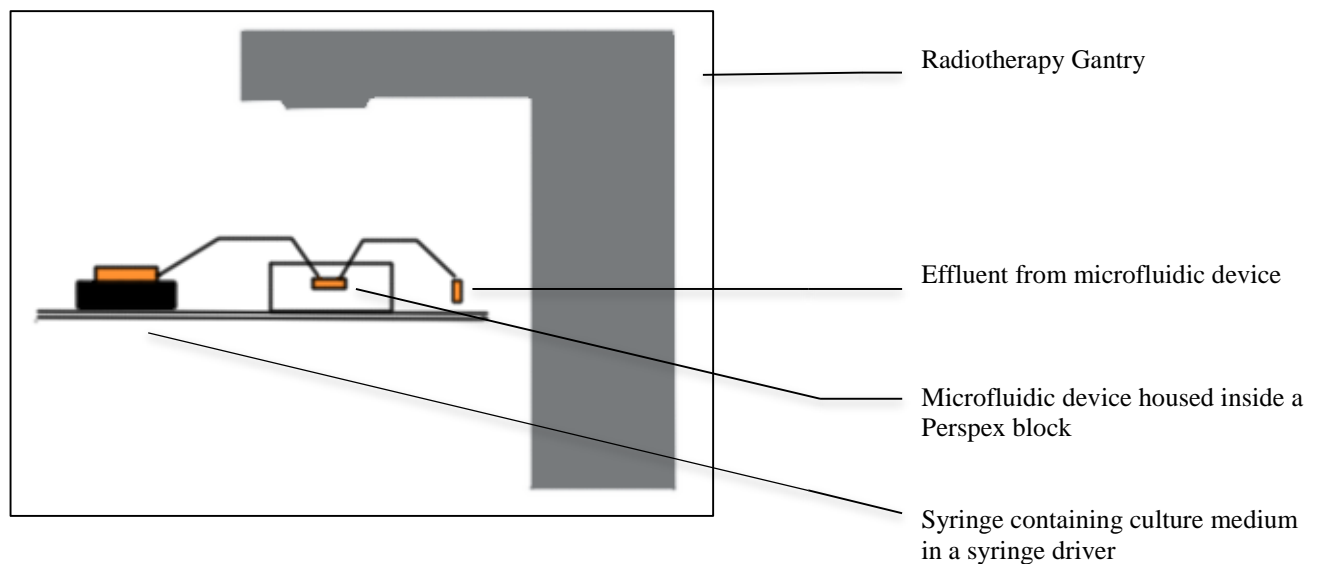


Figure 1a. Schematic diagram demonstrating how the tissue was irradiated whilst being incubated in the microfluidic device.

Figure 1b. Photograph demonstrating how the tissue was irradiated whilst being incubated in the microfluidic device.

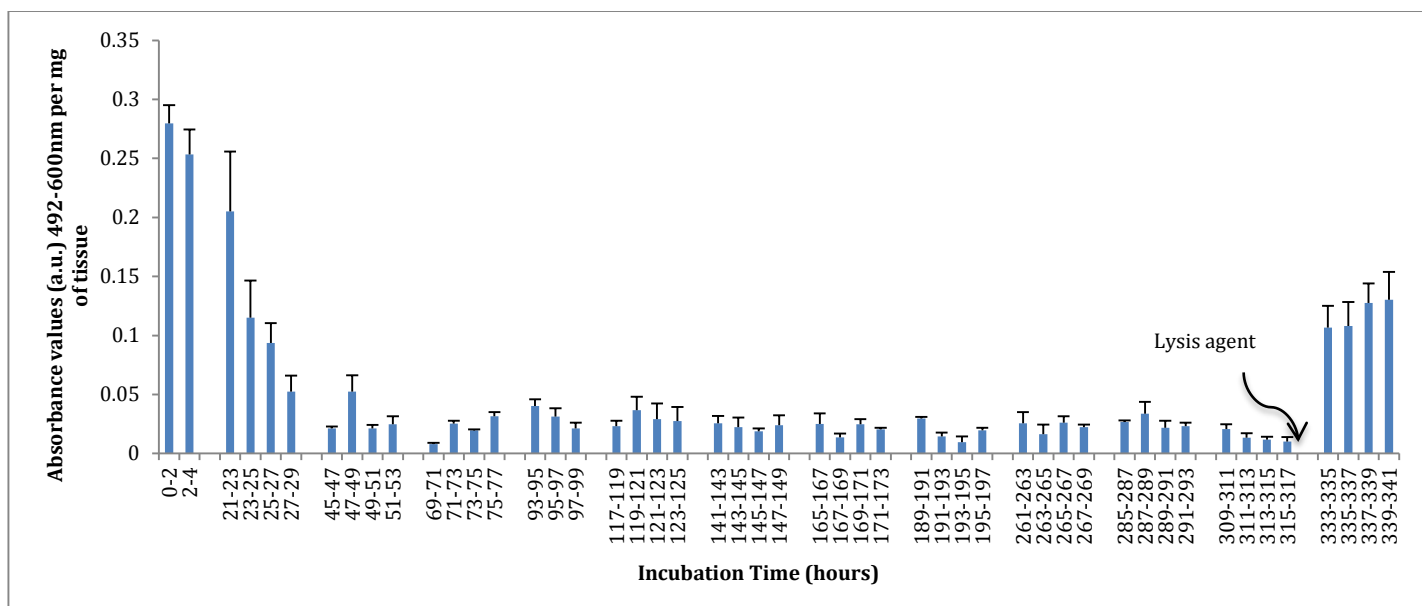


Figure 2. Absorbance measurements following LDH assays on effluent from rat liver maintained in a microfluidic device for 341 h, standardised per mg of tissue (Mean of three experiments + SD). Lysis agent added at 333 h.

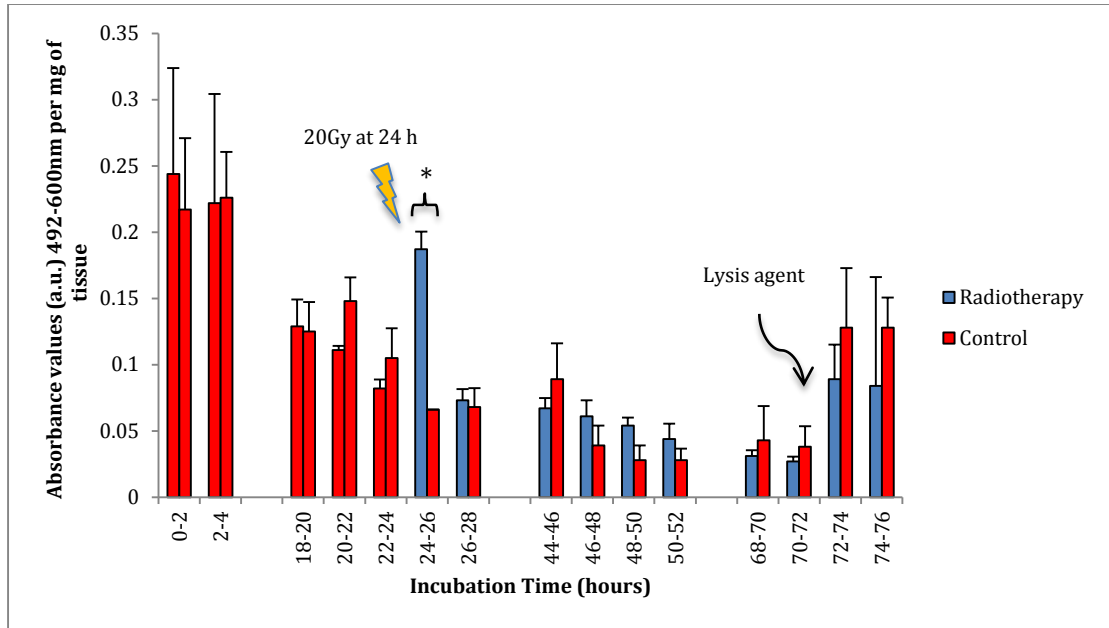


Figure 3. Absorbance measurements following LDH assays on effluent from rat liver standardised per mg of tissue (Mean of three experiments + SD). Single dose of 20Gy administered at 24 h. Lysis agent was added at 70 h. Significant LDH surge demonstrated after the administration of 20Gy compared to the control $p=0.02^*$ unpaired t-test.

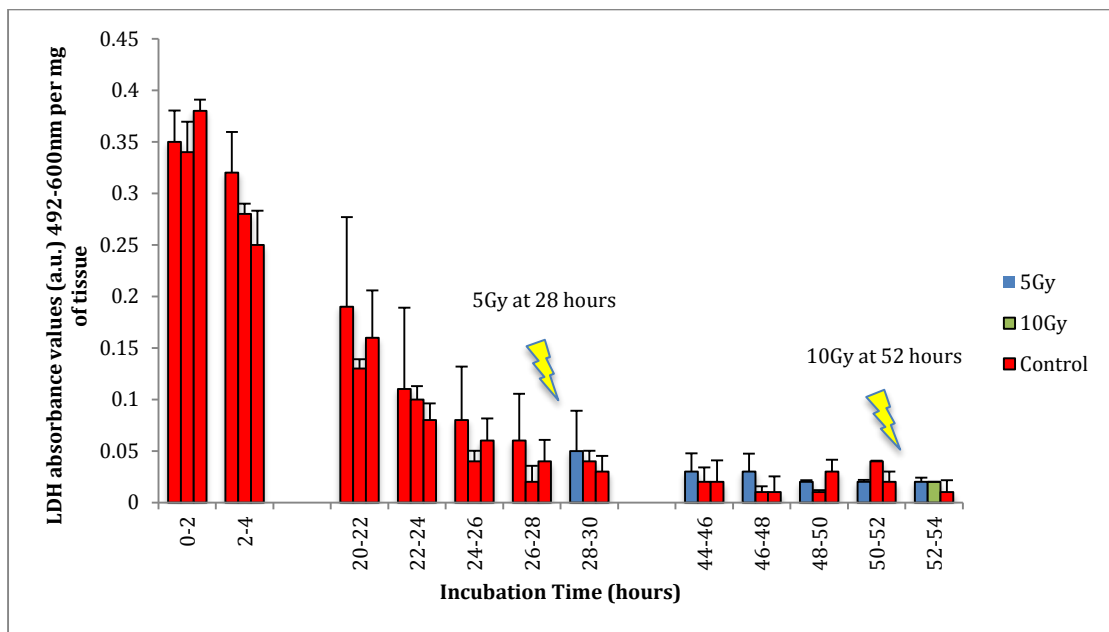
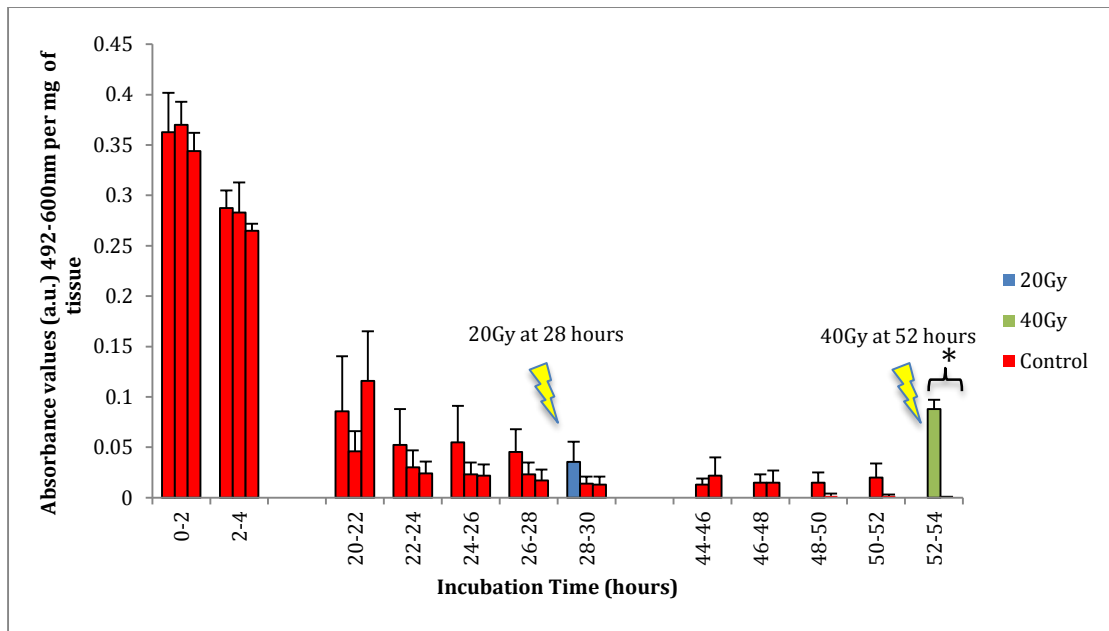


Figure 4a & 4b. Absorbance measurements following LDH assays on effluent from HNSCC tissue standardised per mg of tissue (Mean of three separate experiments + SD). Single doses of 20Gy at 28 h, 40Gy at 52 h (**Figure 4a**); 5Gy at 28 h, 10Gy at 52 h (**Figure 4b**). No radiotherapy to control. No lysis agent. Significant LDH surge demonstrated after administration of 40Gy cf. control t-test $p=0.01^*$.

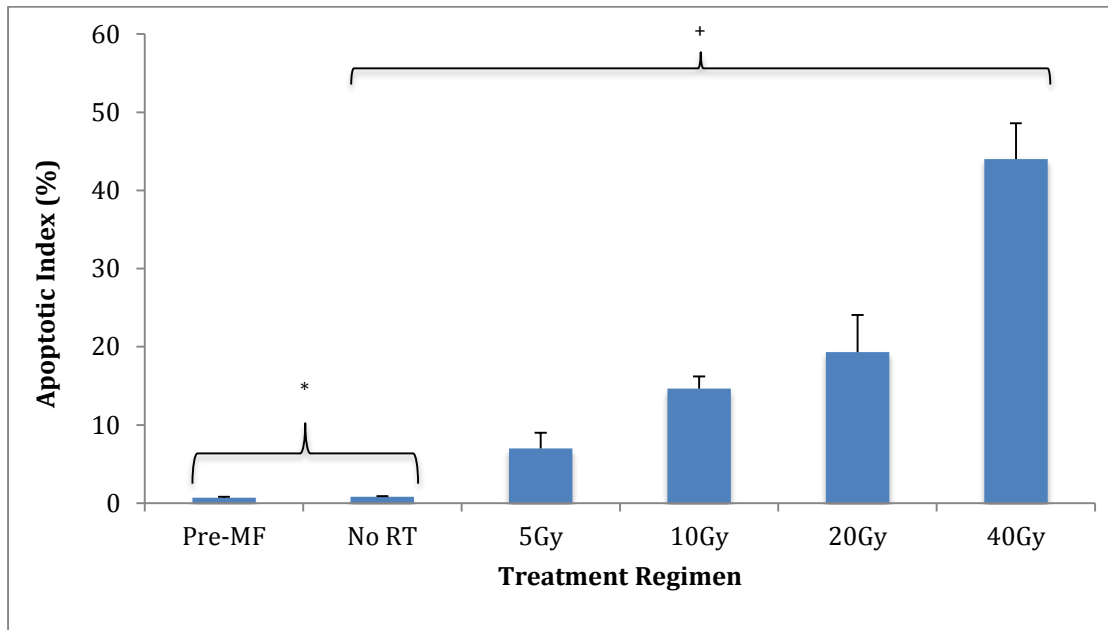
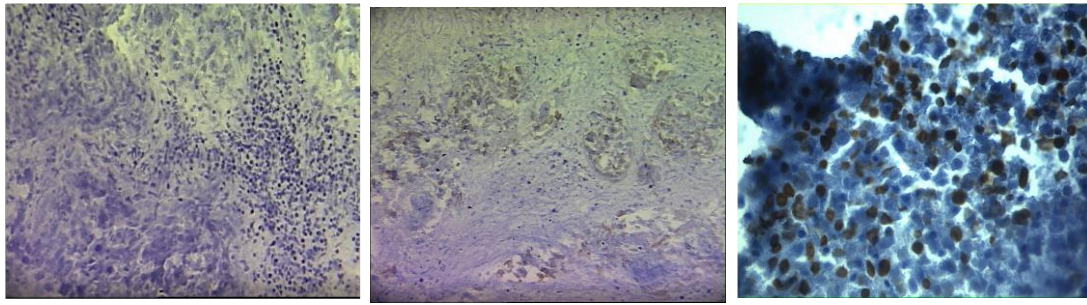


Figure 5a. Immunohistochemical staining of caspase cleaved cytokeratin with M30 (1:100 dilution) in HNSCC. Blue hematoxylin counterstain. Left to right: No radiotherapy (200x magnification), single fraction of 10Gy (200x magnification) and single fraction of 40Gy (400x magnification).

Figure 5b. AI for different treatment regimens in HNSCC treated with single doses of radiotherapy (Mean of three separate experiments + SD). ‘Pre-MF’: tissue not incubated in the microfluidic device or treated with radiotherapy; ‘No RT’: tissue that was incubated in the device for the same duration as the treated tissue, but did not receive radiotherapy treatment. There was no significant difference between the AI of the ‘Pre-MF’ and ‘No RT’ $p=0.29^*$, but there was a significant difference between the AI of the irradiated and non-irradiated tissues $p=0.006^+$ unpaired t-test.

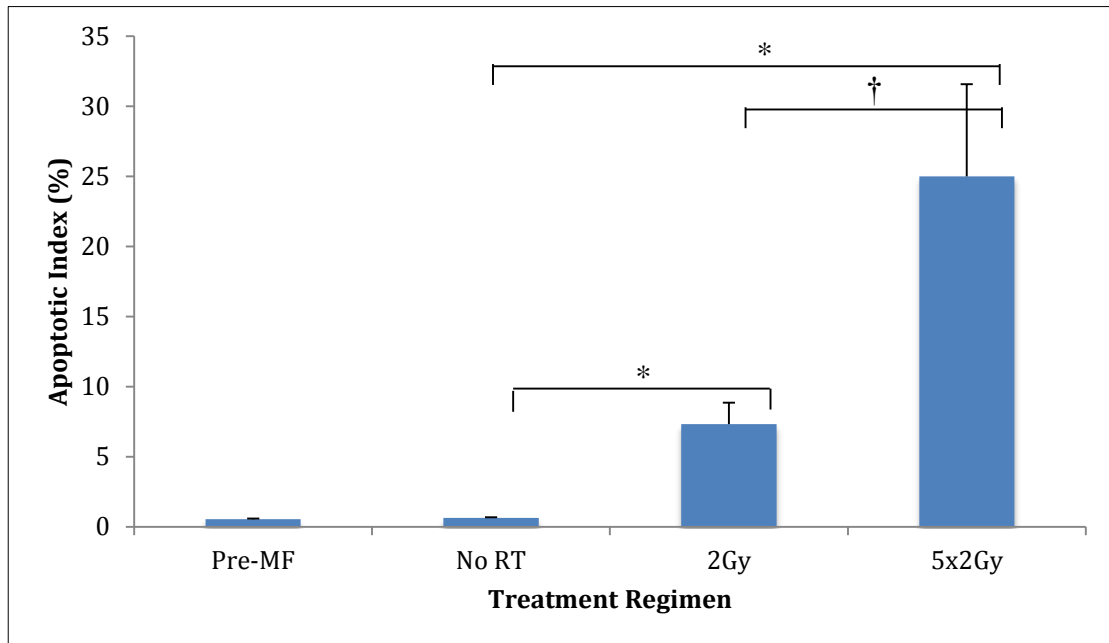
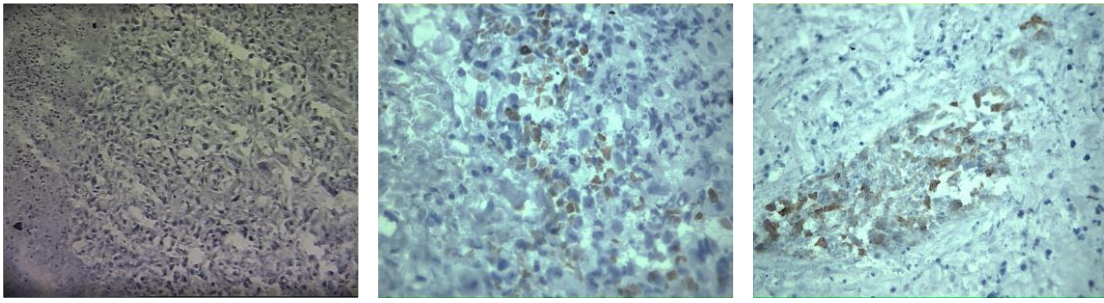


Figure 6a. Immunohistochemical staining of HNSCC with M30 Cytodeath antibody (1:100 dilution) Blue hematoxylin counterstain. Left to right: No RT (200x), single fraction of 2Gy (400x) and 5x2Gy (400x).

Figure 6b. AI for different treatment regimens of HNSCC treated with a single 2Gy dose and a fractionated course (5x2Gy) (Mean of three separate experiments + SD). ‘Pre-MF’ as **Figure 5b**; ‘No RT’ as **Figure 5b**. Significant differences in AI between ‘No RT’ and 2Gy $p=0.002^*$ and between 2Gy and 5x2Gy $p=0.01^\dagger$ unpaired t-test.